Soft Matter

PAPER

View Article Online
View Journal | View Issue

Cite this: *Soft Matter*, 2016, **12**, 3737

Dynamics of flexible active Brownian dumbbells in the absence and the presence of shear flow

Roland G. Winkler

Received 8th December 2015,
Accepted 26th February 2016

DOI: 10.1039/c5sm02965a

www.rsc.org/softmatter

The dynamical properties of a flexible dumbbell composed of active Brownian particles are analytically analyzed. The dumbbell is considered as a simplified description of a linear active polymer. The two beads are independently propelled in directions which change in a diffusive manner. The relaxation behavior of the internal degree of freedom is tightly coupled to the dumbbell activity. The latter dominates the dynamics for strong propulsion. As is shown, limitations in bond stretching strongly influence the relaxation behavior. Similarly, under shear flow, activity determines the relaxation and tumbling behavior at strong propulsion. Moreover, shear leads to a preferred alignment and consequently to shear thinning. Thereby, a different power-law dependence on the shear rate compared to passive dumbbells under flow is found.

1 Introduction

The constituents of active matter convert internal chemical energy or utilize energy from their environment for their propulsion.[1] The resulting nonequilibrium dynamical behavior gives rise to rich physical phenomena, such as swarming,[2–6] turbulence,[5] activity-induced clustering, and phase transitions.[7–20] The spectrum of biologically active systems is wide and ranges from moving bacteria,[1,21,22] the cytoskeleton in living cells[22–31] to the macroscopic scale of flocks of birds and mammalian herds.[32] For synthetically active particles, chemical or physical propulsion mechanisms are exploited for spherical colloids[8,33–35] or objects of other shapes.[35,36] Various propulsion strategies are realized in nature. Bacteria are typically propelled by one or several flagella.[1,2,4,21,37] In the cytoskeleton, actin filaments are driven forward by myosin motors.[27–31,38] Similarly, *in vitro* experiments demonstrate propulsion of microtubules by surface-bound dyneins.[39]

Various active systems exhibit not only common features, but also distinct differences. From a theoretical point of view, the challenge is to find an adequate description for a particular class of systems, which captures their main characteristics. In a rather generic model, the activity-induced hydrodynamic flow field of a microswimmer is described by a force dipole.[5,40,41] Indeed, experiments, theoretical calculations, and simulations for *E. coli* bacteria[5,42–45] and *Chlamydomonas reinhardtii* algae[42,43,46,47] confirm such a description for the far-field flow. However, the near-field flow is rather complex.[42,43,45–47]

Neglecting hydrodynamics completely, various fundamental aspects of microswimmers are captured by their description as active Brownian particles (ABPs).[7,15,16,20,33,48,49] This stochastic model provides fascinating self-organized structures induced by propulsion and excluded-volume interactions.[7,15,16,20,49] Moreover, it is a valuable theoretical model to gain insight into the nonequilibrium statistical properties of active Brownian systems.[50–58] Excluded-volume interactions are of paramount importance for collective phenomena in motility assays and active gels (cytoskeleton). The high aspect ratio of actin filaments or microtubules leads to the alignment of interacting units. These "alignment interactions" can be captured in various ways. Originally, an alignment rule depending on the preferred propulsion direction of some neighborhood of an active particle has been introduced.[32,59] Alternatively, semiflexible of rodlike polymers can be studied directly.[60–65]

Propelled flexible and semiflexible polymeric structures are particular interesting systems, because of the intriguing coupling of their conformations and the activity. Correspondingly, various aspects of active polymers have been studied theoretically and by computer simulations. The linear viscoelastic response of an entangled, isotropic solution of polar semiflexible polymers has been investigated in ref. 66 and, *e.g.*, a novel time dependent power-law regime for the shear modulus is obtained. Other aspects, such as activity-induced ring closer,[67] emerging beat patterns,[68] and collective phenomena,[63] have been studied. The intramolecular dynamics has been addressed,[64] and activity induced aggregation of individual polymers in two dimensions.[65] Hydrodynamic interactions have been taken into account explicitly in the studies of ref. 69 and 70 to elucidate their influence on the polymer conformational properties. Specifically, activity driven oscillations and beating patterns of the semiflexible polymer are found. The influence of hydrodynamic interactions on the dynamics of two driven polymers has been considered in ref. 71.

An analytical description of the dynamics of an active polymer with its (infinitely) many degrees of freedom may be

Theoretical Soft Matter and Biophysics, Institute for Advanced Simulation, Forschungszentrum Jülich, D-52425 Jülich, Germany. E-mail: r.winkler@fz-juelich.de

rather challenging. Here, a simpler approach by adopting a dumbbell model as a first step in understanding the specificities of polymers can be very useful. Dumbbells are indeed used to describe the motion of active particles, typically as a model for a force dipole. Thereby, hydrodynamic interactions are taken into account,[72–74] or the dumbbells are modelled as active Brownian objects.[75–77] Simulation studies of such systems show collective effects[72] and phase transitions.[76,78]

The Brownian dumbbells considered in the literature are typically driven along the connecting bond. In terms of an active polymer, this description is more adequate for a rodlike rather than a flexible or semiflexible polymer. For the latter, the conformational degrees of freedom will lead to a misalignment of the direction of the driving forces along the polymer. This is independent of the local propulsion mechanism, whether it is parallel to the local tangent,[65,68,71] perpendicular to it,[66] or even random.[63,64]

For passive systems, dumbbells are traditionally and successfully applied to describe the dynamical[79] and rheological properties of polymers.[79–82] The two beads might be considered as the polymer ends. The dumbbell bond mimics the conformational properties of the polymer. A rodlike polymer is described by a rigid bond.[79] Flexibility can be implemented in different ways, either by a completely flexible (Gaussian, Hookian) bond, a finitely extensible nonlinear elastic (FENE) bond,[79,83] or by a macroscopic constraint of a constant mean square bond length.[83,84] The latter yields exactly the same force–extension relation as the FENE dumbbell,[83,84] and is an established mean-field approach for polymers.[82–90]

In this article, the dynamical and rheological properties of a flexible active Brownian dumbbell (ABDB) are studied by an analytical approach as a minimal model for a flexible polymer. Thereby, each of the two beads is considered as an active Brownian particle. The emphasize is on the dynamical and rheological dumbbell properties due to the intimate coupling of its entropic degrees of freedom with the activity of the beads and an external shear flow. The diffusive motion of the propulsion velocity of the beads is described by an independent Gaussian, but non-Markovian process. The bond length fluctuates to some extend, but its mean square length is maintained at a prescribed value. The linear stochastic Langevin equation of motion of the bond vector can be solved analytically. In addition, an expression for the conditional probability distribution function can be provided due to the Gaussian nature of the stochastic process. We demonstrate that the relaxation behavior of the bond vector strongly depends on the activity, giving rise to time regimes, which are not present in passive systems. Thereby, activity leads to a faster decay of correlation functions, especially at large propulsion velocities. An applied shear flow implies a shear rate dependent relaxation time, which decreases with increasing shear rate. Hence, activity leads to a speed-up of the dynamics. This is reflected in the bond vector correlation function, which depends on the activity and shear rate. As for passive polymers, shear leads to a preferred bond vector alignment with respect to the flow and correspondingly to shear thinning. Both the alignment angle and the viscosity show a distinctively stronger dependence on the shear rate compared to that of passive dumbbells and asymptotically decay with a different power-law than passive systems. Hence, the calculations shed light on the coupling of the polymer entropic degrees of freedom, activity, and shear flow.

This paper is organized as follows. In Section 2, the model of an active Brownian dumbbell is introduced. The solution of the equations of motion is presented in Section 3, and the dependence of the relaxation time and the bond vector correlation function on the activity is discussed. The dynamics of the ABDB under shear flow is analyzed in Section 4. The dependence of the relaxation time and the bond-vector correlation function on the activity and the shear rate is analyzed. In addition, rheological properties are addressed, specifically the shear induced ABDB alignment and its shear-thinning behavior. To underline the differences between an entropy elastic dumbbell with the constraint of a constant mean square bond length and a purely enthalpic harmonic dumbbell, various results for the latter are presented in Section 5. Finally, Section 6 summarizes the findings. The Appendix illustrates the calculation of averages and correlation functions.

2 Active dumbbell model

As stressed in the Introduction, we are interested in the dynamical properties of active flexible polymers. In a simple, least degree of freedom description, a polymer can be described as an elastic dumbbell, *i.e.*, by two connected beads. To add activity, the two beads are considered as active Brownian particles (ABPs). The internal entropic (conformational) degrees of freedom of the polymer are captured by the harmonic bond potential

$$U = \lambda k_{\mathrm{B}} T \boldsymbol{R}^2, \tag{1}$$

where $\boldsymbol{R} = \boldsymbol{r}_2 - \boldsymbol{r}_1$ is the bond vector between the ABPs at the positions $\boldsymbol{r}_i$ ($i = 1, 2$), T is the temperature, k_{B} is the Boltzmann constant, and λ is a Lagrangian multiplier. The latter ensures that the constraint of a constant mean squared bond length

$$\langle (\boldsymbol{r}_2 - \boldsymbol{r}_1)^2 \rangle = \langle \boldsymbol{R}^2 \rangle = l^2 \tag{2}$$

is fulfilled (*cf.* remarks in the Introduction). The length l is referred to as the dumbbell length. The constraint captures an important aspect of a polymer, namely its limited extensibility.[82–84,87–89] Under equilibrium conditions, the Lagrangian multiplier follows from the partition function as $\lambda_0 = 3/2l^2$ and a Gaussian bond vector distribution is obtained.[82–84]

The overdamped equations of motion of the active dumbbell are

$$\frac{\mathrm{d}\boldsymbol{r}_i}{\mathrm{d}t} = \boldsymbol{v}_i - (-1)^i \frac{2\lambda k_{\mathrm{B}} T}{\gamma_{\mathrm{T}}} \boldsymbol{R} + \frac{1}{\gamma_{\mathrm{T}}} \boldsymbol{\Gamma}_i, \tag{3}$$

with the self-propulsion velocities $\boldsymbol{v}_i$ of the ABPs, the forces $\boldsymbol{F}_i = (-1)^i 2\lambda k_{\mathrm{B}} T \boldsymbol{R}/\gamma_{\mathrm{T}}$ due to the bond, and the friction coefficient γ_{T} of the translational motion. The $\boldsymbol{\Gamma}_i(t)$ are Gaussian and Markovian stochastic forces with zero mean and the moments

$$\langle \Gamma_{\alpha,i}(t) \Gamma_{\beta,j}(t') \rangle = 2k_{\mathrm{B}} T \gamma_{\mathrm{T}} \delta_{ij} \delta_{\alpha\beta} (t - t'), \tag{4}$$

$i, j \in \{1, 2\}$ and $\alpha, \beta \in \{x, y, z\}$. The translational friction coefficient is related to the diffusion coefficient D_{T} of an independent ABP *via* $D_{\mathrm{T}} = k_{\mathrm{B}} T/\gamma_{\mathrm{T}}$.

The two ABPs account for the overall activity of the flexible (coiled) polymer. Hence, we assume that the self-propulsion velocities of the ABPs are independent and describe them by the equations of motion

$$\frac{\mathrm{d}\boldsymbol{v}_i}{\mathrm{d}t} = -\gamma_\mathrm{R}\boldsymbol{v}_i + \boldsymbol{\eta}_i, \tag{5}$$

where $\boldsymbol{\eta}_i(t)$ are Gaussian and Markovian stochastic forces with the zero mean and the moments

$$\langle \boldsymbol{\eta}_i(t)\cdot\boldsymbol{\eta}_j(t')\rangle = 2(d-1)D_\mathrm{R}{v_0}^2\delta_{ij}\delta(t-t'), \tag{6}$$

with the rotational diffusion coefficient $D_\mathrm{R} = \gamma_\mathrm{R}/(d-1)$, the damping factor γ_R, the magnitude v_0 of the propulsion velocity (activity), and the dimension d. Here, $d = 3$ will be considered. In contrast to the often applied approach $\boldsymbol{v}_i = v_0\boldsymbol{e}_i$,[7,15,16,20,58] with a constant self-propulsion velocity v_0 and the unit vector $\boldsymbol{e}_i$ of the propulsion direction, the magnitude of the velocity $\boldsymbol{v}_i$ is non-constant.[1] However, the second moment (6) ensures that $\langle \boldsymbol{v}_i^2\rangle = {v_0}^2$. We like to point out that the fluctuations $\boldsymbol{\eta}_i$ are not necessarily thermal. Activity can cause larger rotational diffusion coefficients than thermal noise, which has been confirmed experimentally for *E. coli* bacteria[1,5,91,92] and *Chlamydomonas reinhardtii* cells.[5]

The equations of motion (5) for the propulsion velocities are decoupled from eqn (3), and their solutions are

$$\boldsymbol{v}_i(t) = \int_{-\infty}^{t} \mathrm{e}^{-(t-t')}\boldsymbol{\eta}_i(t')\mathrm{d}t', \tag{7}$$

in the stationary state. Since the correlation functions are given by

$$\langle \boldsymbol{v}_i(t)\cdot\boldsymbol{v}_j(t')\rangle = \delta_{ij}{v_0}^2\mathrm{e}^{-\gamma_\mathrm{R}|t-t'|}, \tag{8}$$

it suffices to consider eqn (3) only, with $\boldsymbol{v}_i$ as Gaussian but non-Markovian processes with zero mean.[16,64,93] We like to point out that the correlation function eqn (8) follows similarly from the equation of motion $\mathrm{d}\boldsymbol{e}_i(t)/\mathrm{d}t = \boldsymbol{e}_i(t)\times\boldsymbol{\eta}_i(t)$ of the unit orientation vector $\boldsymbol{e}$ with the appropriate choice of the random forces $\boldsymbol{\eta}_i$.[58] Hence, the equation of motion eqn (5) yields the same correlation function [eqn (8)] for an isotropic system as that for the propulsion velocity with the unit vector $\boldsymbol{e}$. Thus, the same results are obtained for $\boldsymbol{v}$ independent of the underlaying dynamics. In the following, we will work with the correlation function eqn (8).

3 Dynamics of the active dumbbell

3.1 Center of mass motion

The equation of motion of the center of mass $\boldsymbol{r}_\mathrm{cm} = (\boldsymbol{r}_1 + \boldsymbol{r}_2)/2$ of a dumbbell is

$$\frac{\mathrm{d}\boldsymbol{r}_\mathrm{cm}}{\mathrm{d}t} = \boldsymbol{v}_\mathrm{cm} + \frac{1}{\gamma_\mathrm{T}}\boldsymbol{\Gamma}_\mathrm{cm}, \tag{9}$$

with the abbreviations $\boldsymbol{v}_\mathrm{cm} = (\boldsymbol{v}_1 + \boldsymbol{v}_2)/2$ and $\boldsymbol{\Gamma}_\mathrm{cm} = (\boldsymbol{\Gamma}_1 + \boldsymbol{\Gamma}_2)/2$. The center-of-mass mean square displacement (MSD) in three dimensions ($d = 3$) is then given by the well-known expression[1,33,34,77,93]

$$\left\langle (\boldsymbol{r}_\mathrm{cm}(t) - \boldsymbol{r}_\mathrm{cm}(0))^2\right\rangle = \frac{3k_\mathrm{B}T}{\gamma_\mathrm{T}}t + \frac{2{v_0}^2}{{\gamma_\mathrm{R}}^2}(\gamma_\mathrm{R}t + \mathrm{e}^{-\gamma_\mathrm{R}t} - 1). \tag{10}$$

For $\gamma_\mathrm{R}t \ll 1$, the MSD reduces to $\langle(\boldsymbol{r}_\mathrm{cm}(t) - \boldsymbol{r}_\mathrm{cm}(0))^2\rangle = 3k_\mathrm{B}Tt/\gamma_\mathrm{T} + {v_0}^2t^2$, *i.e.*, a linear diffusive contribution by the Brownian motion of the dumbbell and an activity-induced ballistic motion. In the limit $\gamma_\mathrm{R}t \gg 1$, the diffusion coefficient is $D = D_\mathrm{T}/2 + {v_0}^2/6D_\mathrm{R}$. Compared to the diffusion coefficient of an individual ABP, naturally only half of the Brownian diffusion coefficient appears. However, the activity-induced diffusion is identical to that of an individual ABP. A detailed discussion of the center-of-mass mean square displacement is presented in ref. 78.

3.2 Bond vector dynamics

The equation of motion for the bond vector is given by

$$\frac{\mathrm{d}\boldsymbol{R}}{\mathrm{d}t} = -\frac{4\lambda k_\mathrm{B}T}{\gamma_\mathrm{T}}\boldsymbol{R} + \Delta\boldsymbol{v} + \frac{1}{\gamma_\mathrm{T}}\Delta\boldsymbol{\Gamma}. \tag{11}$$

Here, we use the terms $\Delta\boldsymbol{v} = \boldsymbol{v}_2 - \boldsymbol{v}_1$ and $\Delta\boldsymbol{\Gamma} = \boldsymbol{\Gamma}_2 - \boldsymbol{\Gamma}_1$. The linear equation is easily solved,[93] and we find

$$\boldsymbol{R}(t) = \boldsymbol{R}_0\mathrm{e}^{-t/\tau} + \int_0^t \mathrm{e}^{-(t-t')/\tau}\left(\Delta\boldsymbol{v}(t') + \frac{1}{\gamma_\mathrm{T}}\Delta\boldsymbol{\Gamma}(t')\right)\mathrm{d}t', \tag{12}$$

with the relaxation time

$$\tau = \frac{\gamma_\mathrm{T}}{4\lambda k_\mathrm{B}T} \tag{13}$$

and the initial bond vector $\boldsymbol{R}_0$ at time $t = 0$. Since our stochastic processes are Gaussian, we can (in principle) calculate all desired moments from the solution eqn (12).

Even more, the conditional probability distribution $\psi(\boldsymbol{R},t;\boldsymbol{R}_0,0)$ can be given due to the Gaussian nature of the processes and despite the non-Markovian character of $\Delta\boldsymbol{v}_i$.[94] Explicitly, the distribution function reads

$$\psi(\boldsymbol{R},t;\boldsymbol{R}_0,0) = \left(\frac{3}{2\pi\langle\Delta\boldsymbol{R}^2\rangle}\right)^{3/2}\exp\left(-3(\boldsymbol{R} - \langle\boldsymbol{R}\rangle)^2\Big/2\langle\Delta\boldsymbol{R}^2\rangle\right), \tag{14}$$

with the average $\langle\boldsymbol{R}\rangle = \boldsymbol{R}_0\mathrm{e}^{-t/\tau}$ and the mean square displacement $\langle\Delta\boldsymbol{R}^2\rangle = \langle(\boldsymbol{R}(t) - \boldsymbol{R}(0))^2\rangle$. In the stationary state $t \to \infty$, the distribution function turns into a Gaussian with the zero mean and, as required by the constraint (2), the width $\langle\boldsymbol{R}^2\rangle = l^2$.

3.3 Lagrangian multiplier—relaxation time

In order to determine the Lagrangian multiplier to satisfy eqn (2), the mean square bond vector is required. Using eqn (12), we find

$$\langle\boldsymbol{R}^2\rangle = \frac{6k_\mathrm{B}T}{\gamma_\mathrm{T}}\tau + \frac{2{v_0}^2}{1+\gamma_\mathrm{R}\tau}\tau^2 \tag{15}$$

in the stationary state (*cf.* Appendix A for a more detailed calculation). Setting $\langle\boldsymbol{R}^2\rangle = l^2$, we obtain

$$\tau = \frac{l^2\gamma_\mathrm{T}\gamma_\mathrm{R} - 6k_\mathrm{B}T + \sqrt{(6k_\mathrm{B}T + l^2\gamma_\mathrm{T}\gamma_\mathrm{R})^2 + 8l^2{\gamma_\mathrm{T}}^2{v_0}^2}}{12k_\mathrm{B}T\gamma_\mathrm{R} + 4{v_0}^2\gamma_\mathrm{T}}. \tag{16}$$

The Lagrangian multiplier itself follows *via* eqn (13). The relaxation time and λ depend in a complex manner on the self-propulsion velocity, an aspect neglected in the analytical studies of the Gaussian polymer of ref. 95. The inextensibility property of a polymer leads to bond forces, which depend on

self-propulsion and strongly affect the relaxation behavior. This is expressed, in our mean-field description by eqn (16). Introducing the Péclet number[1,13,51]

$$\mathrm{Pe} = \frac{v_0}{l D_\mathrm{R}} \tag{17}$$

and the abbreviation

$$\Delta = \frac{D_\mathrm{T}}{l^2 D_\mathrm{R}} \tag{18}$$

for the ratio of the diffusion coefficients, the equation for the Lagrangian multiplier $\mu = \lambda/\lambda_0$ becomes

$$\frac{\tau}{\tau_0} = \frac{1}{\mu} = 3\Delta \frac{1 - 3\Delta + \sqrt{(1+3\Delta)^2 + 2\mathrm{Pe}^2}}{6\Delta + \mathrm{Pe}^2}, \tag{19}$$

with $\tau_0 = \gamma_\mathrm{T} l^2/6k_\mathrm{B}T$ being the relaxation time of a passive dumbbell. In the asymptotic limit $\Delta \to 0$, *i.e.*, the rotational diffusion coefficient is much larger than that for translational motion, eqn (19) yields

$$\mu = \frac{\mathrm{Pe}^2}{3\Delta\left(1 + \sqrt{1 + 2\mathrm{Pe}^2}\right)}. \tag{20}$$

For $\mathrm{Pe} \gg 1$, the expression (20) reduces to $\mu = \mathrm{Pe}/3\sqrt{2}\Delta$. Evidently, the bond force increases with increasing rotational diffusion coefficient and increasing Péclet number. Without propulsion (Pe = 0), eqn (19) yields $\mu = 1$.

Fig. 1 displays Lagrangian multipliers as a function of Pe for various values of Δ. We assume that the rotational diffusion coefficient D_R is equal to or larger than the thermal value. Hence, we use $\Delta \leq 1$. The individual curves are well described by the analytical expression (20) for large Péclet numbers. For large Δ values, μ increases essentially linearly with the Péclet number ($\mathrm{Pe} \gtrsim 10$). However, for $\Delta \lesssim 10^{-2}$, there exists an intermediate regime, where μ increases approximately quadratically with Pe ($\mathrm{Pe} < 1$). We like to emphasize that the increase of μ with increasing Péclet number is a consequence of the constraint (2). Without such an condition, the Lagrangian multiplier would be equal to unity and independent of the activity. Thus, such a model would miss an essential aspect of polymers, namely their finite extensibility.

The relaxation time is conveniently scaled by the friction coefficient γ_R. Hence,

$$\gamma_\mathrm{R}\tau = \frac{1 - 3\Delta + \sqrt{(3\Delta+1)^2 + 2\mathrm{Pe}^2}}{6\Delta + \mathrm{Pe}^2}. \tag{21}$$

In the limit Pe = 0, *i.e.*, $v_0 = 0$, this expression yields the Lagrangian multiplier $\lambda_0 = 3/2l^2$. Moreover, for $\Delta = 0$, *i.e.*, zero translational friction, we find

$$\gamma_\mathrm{R}\tau = \frac{1 + \sqrt{1 + 2\mathrm{Pe}^2}}{\mathrm{Pe}^2}. \tag{22}$$

This expression reduces to $\gamma_\mathrm{R}\tau = \sqrt{2}/\mathrm{Pe}$ in the limit $\mathrm{Pe} \to \infty$. Thus, the relaxation time $\tau = l/\sqrt{2}v_0$ approaches zero for $v_0 \to \infty$.

The dependence of the relaxation time on the Péclet number is presented in Fig. 2 for various ratios Δ. Since the activity dependence of τ is completely governed by the Lagrangian multiplier, the figure exhibits the same features as Fig. 1. In the asymptotic limit of large Péclet numbers, $\gamma_\mathrm{R}\tau$ decreases as 1/Pe. For $\mathrm{Pe} < 1$ and small Δ, there is an intermediate regime, where $\gamma_\mathrm{R}\tau$ decreases as $1/\mathrm{Pe}^2$ with increasing Pe. In the asymptotic limit $\Delta \to 0$, the functional dependence on Pe is captured by eqn (22).

Fig. 1 and 2 reflect the tight coupling between the entropic degrees of freedom of a polymer, its finite extensibility, and activity, an aspect specific to polymers with their internal conformational degrees of freedom.

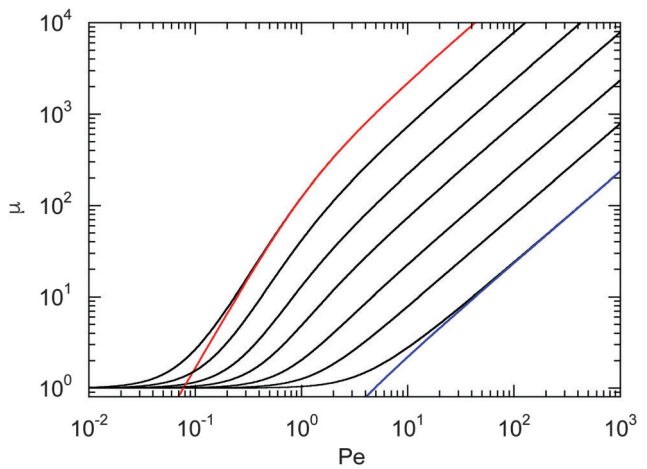

Fig. 1 Lagrangian multiplier $\mu = \lambda/\lambda_0$ [eqn (19)] as a function of Péclet number for the diffusion coefficient ratios $\Delta = D_\mathrm{T}/l^2 D_\mathrm{R} = 10^{-3}$, 3×10^{-3}, 10^{-2}, 3×10^{-2}, 10^{-1}, 0.3, and 1 (left to right). The colored lines (left and right) correspond to the approximation of eqn (20) with the respective value of Δ.

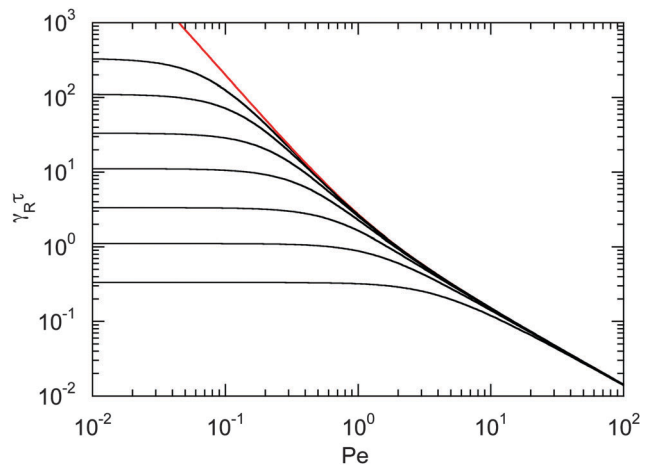

Fig. 2 Scaled dumbbell relaxation times $\gamma_\mathrm{R}\tau$ [eqn (21)] as a function of Péclet number for the diffusion coefficient ratios $\Delta = D_\mathrm{T}/l^2 D_\mathrm{R} = 10^{-3}$, 3×10^{-3}, 10^{-2}, 3×10^{-2}, 10^{-1}, 0.3, and 1 (top to bottom). The red line correspond to the approximation of eqn (22).

3.4 Bond vector autocorrelation function

The dynamics of the bond vector can be characterized by the correlation function

$$\langle \boldsymbol{R}(t)\cdot\boldsymbol{R}(0)\rangle = l^2 \mathrm{e}^{-t/\tau} + \frac{2v_0^2\tau^2}{1-(\gamma_\mathrm{R}\tau)^2}\left(\mathrm{e}^{-\gamma_\mathrm{R}t} - \mathrm{e}^{-t/\tau}\right), \qquad (23)$$

which is straightforwardly obtained as illustrated in Appendix A. In terms of the Péclet number (17), the correlation function reads

$$\langle \boldsymbol{R}(t)\cdot\boldsymbol{R}(0)\rangle = l^2 \mathrm{e}^{-t/\tau}\left(1 - \frac{(\gamma_\mathrm{R}\tau)^2\mathrm{Pe}^2}{2\left(1-(\gamma_\mathrm{R}\tau)^2\right)}\right) + \frac{l^2(\gamma_\mathrm{R}\tau)^2\mathrm{Pe}^2}{2\left(1-(\gamma_\mathrm{R}\tau)^2\right)}\mathrm{e}^{-\gamma_\mathrm{R}t}. \qquad (24)$$

There are two exponentially decaying contributions to the correlation function, a contribution with the relaxation time τ, which strongly depends on the activity, and a contribution comprising γ_R, where the exponent is independent of self-propulsion. In the asymptotic limit $\mathrm{Pe} \to \infty$, $\gamma_\mathrm{R}\tau = \sqrt{2}/\mathrm{Pe} \ll 1$ and the correlation function reduces to

$$\langle \boldsymbol{R}(t)\cdot\boldsymbol{R}(0)\rangle = l^2 \mathrm{e}^{-\gamma_\mathrm{R}t}. \qquad (25)$$

Here, the decay of the correlation function is independent of the propulsion force and solely governed by the orientational dynamics of the ABPs. This is similar to a rodlike active object propelled along its director, which changes by Brownian diffusion. In the previously addressed intermediate Pe regime, $\gamma_\mathrm{R}\tau$ can be approximated by $\gamma_\mathrm{R}\tau = 2/\mathrm{Pe}^2$, which is much larger than unity for $\mathrm{Pe} < 1$ (*cf.* Fig. 2), hence,

$$\langle \boldsymbol{R}(t)\cdot\boldsymbol{R}(0)\rangle = l^2 \mathrm{e}^{-t/\tau}\left(1+\frac{\mathrm{Pe}^2}{2}\right) - \frac{\mathrm{Pe}^2 l^2}{2}\mathrm{e}^{-\gamma_\mathrm{R}\tau(t/\tau)} \approx l^2 \mathrm{e}^{-t/\tau}\left(1+\frac{\mathrm{Pe}^2}{2}\right). \qquad (26)$$

The correlation function decays with the relaxation time τ, which strongly depends on Pe (*cf.* remarks at the end of Section 3.3). In the limit $\mathrm{Pe} \to 0$, the relaxation behavior of a passive dumbbell is obtained.

In the exponentially decaying regimes, we can determine dumbbell-rotational diffusion coefficients D_R^d. With the definition $\langle \boldsymbol{R}(t)\cdot\boldsymbol{R}(0)\rangle \sim \mathrm{e}^{-2D_\mathrm{R}^\mathrm{d}t}$, eqn (25) and (26) imply

$$D_\mathrm{R}^\mathrm{d} = \begin{cases} D_\mathrm{R}, & \mathrm{Pe} \gg 1 \\ \dfrac{D_\mathrm{R}(6\Delta + \mathrm{Pe}^2)}{1-3\Delta+\sqrt{(3\Delta+1)^2+2\mathrm{Pe}^2}}, & 0 < \mathrm{Pe} < 1 \\ 3k_\mathrm{B}T/l^2\gamma_\mathrm{T}, & \mathrm{Pe} = 0 \end{cases}. \qquad (27)$$

Hence, even for a moderate Péclet number, the rotational dynamics of the dumbbell is determined by the activity.

Fig. 3 provides an example of the bond vector correlation function. For the ratio of the diffusion coefficients, we choose $\Delta = 10^{-2}$, assuming that D_R is larger than the thermal value. The correlation function decays exponentially in the limits $\mathrm{Pe} \to \infty$ and $\mathrm{Pe} \to 0$ according to eqn (25) and (26), respectively. The correlation functions decay in a non-exponential manner over a wide range of Péclet numbers including the considered values $\mathrm{Pe} = 0.5-5$. Thereby, the decay is slower than exponential at short times. On longer time scales, the exponential decay is reached according to eqn (25) for $\mathrm{Pe} > 2$ and eqn (26) for $\mathrm{Pe} < 2$. In summary, the coupling of the internal polymer degrees of freedom and activity leads to a complex, in general, non-exponential decay of the bond vector correlation function.

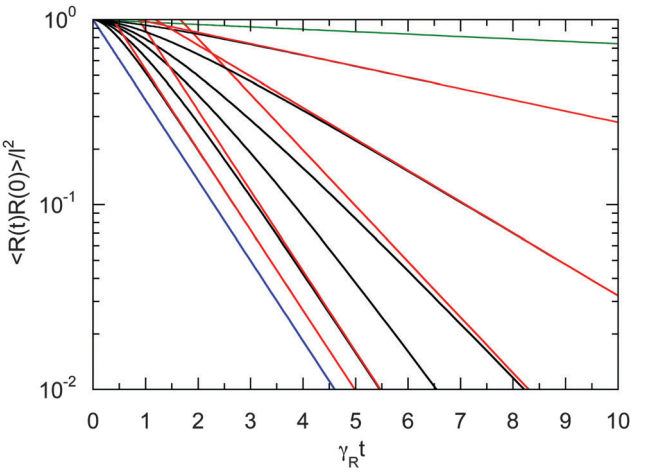

Fig. 3 Bond vector autocorrelation functions of a dumbbell as a function of the scaled time $\gamma_\mathrm{R}t$ for the Péclet numbers Pe = 0 (green), 0.5, 1.0, 1.5, 2.0, 3.0, 5.0, and ∞ (blue) (top to bottom). The diffusion coefficient ratio is set to $\Delta = 10^{-2}$. The red lines correspond to the two exponentially decaying terms of eqn (24). For $\mathrm{Pe} < 2$, the long-time decay is determined by the decay of the first term on the right-hand side of eqn (24) (*cf.* eqn (26)), and for $\mathrm{Pe} > 2$ by the second term (*cf.* eqn (25)).

4 Active dumbbell in shear flow

The nonequilibrium properties of passive Gaussian dumbbells in shear flow have been studied intensively. Various results are presented in ref. 79. Finite extensible Gaussian dumbbells, with the constraint of a constant mean square bond vector, have been studied in ref. 82. In particular, it has been shown that the finite extensibility of dumbbells and polymers is fundamental for shear thinning.[79,82,85] In this section, an extension to active Brownian dumbbells under shear flow is provided.

4.1 Equation of motion

In shear flow with shear rate $\dot\gamma$, the equations of motion eqn (11) become

$$\frac{\mathrm{d}R_\beta}{\mathrm{d}t} = -\frac{1}{\tau_\mathrm{s}}R_\beta + \Delta v_\beta + \frac{1}{\gamma_\mathrm{T}}\Delta\Gamma_\beta + \dot\gamma R_y\delta_{\beta x}. \qquad (28)$$

Flow is along the x-direction and the gradient is along the y-direction of the Cartesian reference frame. Here, the relaxation time $\tau_\mathrm{s} = \gamma_\mathrm{T}/4\lambda_\mathrm{s}k_\mathrm{B}T$ is introduced with the index 's' to indicate the dependence of the relaxation time on the shear rate. Similarly, λ_s

denotes the Lagrangian multiplier in the presence of shear flow. These are linear and independent equations as long as we assume the validity of eqn (5) and the correlation functions

$$\left\langle \eta_{\alpha,i}(t)\eta_{\beta,j}(t')\right\rangle = \frac{2(d-1)}{d} D_{\mathrm{R}} v_0^2 \delta_{ij}\delta_{\alpha\beta}\delta(t-t') \tag{29}$$

in d dimensions. This implies the relation

$$\left\langle v_{\alpha,i}(t)v_{\beta,j}(t')\right\rangle = \delta_{ij}\delta_{\alpha\beta}\frac{v_0^2}{d}\mathrm{e}^{-\gamma_{\mathrm{R}}|t-t'|}, \tag{30}$$

i.e., independent velocity correlations for the Cartesian components, which does not necessarily apply to active systems with a velocity $\boldsymbol{v} = v_0\boldsymbol{e}$, with the unit vector $\boldsymbol{e}$. Here, the Cartesian components are coupled. However, we expect a minor (quantitative) difference between our approach, eqn (28) and (30), where $\langle \boldsymbol{v}^2\rangle = {v_0}^2$, and an approach applying the condition $|\boldsymbol{v}| = v_0$, as long as bond vectors are considered. Under this assumption, the solution of eqn (28) is

$$R_\beta(t) = \int_{-\infty}^{t} \mathrm{e}^{-(t-t')/\tau_{\mathrm{s}}}\left(\Delta v_\beta(t') + \Delta\Gamma_\beta(t') + \dot\gamma R_y(t')\delta_{\beta x}\right)\mathrm{d}t'. \tag{31}$$

4.2 Lagrangian multiplier

The calculation of the mean square bond vector yields (*cf.* Appendix A)

$$\left\langle \boldsymbol{R}^2\right\rangle = \frac{6k_{\mathrm{B}}T}{\gamma_{\mathrm{T}}}\tau_{\mathrm{s}} + \frac{2{v_0}^2}{1+\gamma_{\mathrm{R}}\tau_{\mathrm{s}}}{\tau_{\mathrm{s}}}^2 + \dot\gamma^2\frac{k_{\mathrm{B}}T}{\gamma_{\mathrm{T}}}{\tau_{\mathrm{s}}}^3 + \dot\gamma^2\frac{{v_0}^2(2+\gamma_{\mathrm{R}}\tau_{\mathrm{s}})}{3(1+\gamma_{\mathrm{R}}\tau_{\mathrm{s}})^2}{\tau_{\mathrm{s}}}^4. \tag{32}$$

As usual, we introduce the Weissenberg number[85,96]

$$\mathrm{Wi} = \dot\gamma\tau \tag{33}$$

as a product of the shear rate and the relaxation time at a zero shear rate, which in our active system is τ of eqn (16). In addition, for the sake of brevity, we introduce the Lagrangian multiplier $\mu_{\mathrm{s}} = \lambda_{\mathrm{s}}/\lambda_0 = \tau_0/\tau_{\mathrm{s}}$. Hence, the constraint (2) turns into the condition for μ_{s}

$$\begin{aligned} 1 \;&= \frac{1}{\mu_{\mathrm{s}}} + \frac{\mathrm{Pe}^2}{18\Delta^2\left(1+(3\Delta\mu_{\mathrm{s}})^{-1}\right)}\frac{1}{{\mu_{\mathrm{s}}}^2} + \frac{\mathrm{Wi}^2\mu^2}{6}\frac{1}{{\mu_{\mathrm{s}}}^3} \\ &\quad + \frac{\mathrm{Wi}^2\mathrm{Pe}^2\mu^2\left(2+(3\Delta\mu_{\mathrm{s}})^{-1}\right)}{108\Delta^2\left(1+(3\Delta\mu_{\mathrm{s}})^{-1}\right)^2}\frac{1}{{\mu_{\mathrm{s}}}^4}. \end{aligned} \tag{34}$$

The Lagrangian multiplier μ is the solution of eqn (19) at zero shear.

Eqn (34) yields the following asymptotic dependencies:

- Passive dumbbell (Pe = 0, $\mu = 1$)

$${\mu_{\mathrm{s}}}^3 - {\mu_{\mathrm{s}}}^2 - \frac{\mathrm{Wi}^2}{6} = 0. \tag{35}$$

This is the expression derived in ref. 82.

- $\Delta \to 0$ and $\mathrm{Pe} \ll 1$, or $\mu_{\mathrm{s}}\Delta \ll 1$

$$\left(\frac{\mu_{\mathrm{s}}}{\mu}\right)^3 - \left(\frac{\mu_{\mathrm{s}}}{\mu}\right)^2 - \frac{\mathrm{Wi}^2}{6} = 0. \tag{36}$$

Here, the same equation as for Pe = 0 is obtained, *i.e.*, we find the same dependence on the Weissenberg number as for the passive dumbbell. However, it has to be kept in mind that $\mu = \mathrm{Pe}^2/6\Delta$ in this limit. For $\mathrm{Wi} \gg 1$

$$\mu_{\mathrm{s}} = \mu\frac{\mathrm{Wi}^{2/3}}{\sqrt[3]{6}} = \frac{\mathrm{Pe}^2}{6\Delta}\frac{\mathrm{Wi}^{2/3}}{\sqrt[3]{6}}. \tag{37}$$

Hence, the Lagrangian multiplier depends quadratically on the Péclet number.

- $\Delta < 1$, $\mathrm{Pe} < \infty$, and $\mathrm{Wi} \to \infty$

$$\frac{\mu_{\mathrm{s}}}{\mu} = \frac{\mathrm{Wi}^{2/3}}{(6\mu)^{1/3}}. \tag{38}$$

- $\Delta < 1$, $\mathrm{Pe} \gg 1$, and $\mathrm{Wi} < \infty$

$$\left(\frac{\mu_{\mathrm{s}}}{\mu}\right)^4 - \left(\frac{\mu_{\mathrm{s}}}{\mu}\right)^2 - \frac{\mathrm{Wi}^2}{3} = 0. \tag{39}$$

The solution of this equation is

$$\frac{\mu_{\mathrm{s}}}{\mu} = \frac{1}{\sqrt{2}}\sqrt{1+\sqrt{1+\frac{4}{3}\mathrm{Wi}^2}}, \tag{40}$$

which yields in the asymptotic limit $\mathrm{Wi} \to \infty$

$$\mu_{\mathrm{s}} = \mu\frac{\sqrt{\mathrm{Wi}}}{\sqrt[4]{3}} = \frac{\mathrm{Pe}}{3\sqrt{2}\Delta}\frac{\sqrt{\mathrm{Wi}}}{\sqrt[4]{3}}, \tag{41}$$

i.e., μ_{s} depends linearly on the Péclet number. Note that λ_{s} of an active dumbbell at large Péclet numbers exhibits a qualitative different dependence on the Weissenberg number as a passive dumbbell.

In eqn (36) and (40), the dependence on the Péclet number is solely *via* μ. As shown by the asymptotic expressions (37) and (41), we obtain a crossover from a Pe^2 dependence for $\mathrm{Pe} \ll 1$ to a linear dependence for $\mathrm{Pe} \gg 1$.

Fig. 4 shows Lagrangian-multiplier ratios μ_{s}/μ as a function of the Weissenberg number for $\Delta = 3 \times 10^{-3}$ (a) and $\Delta = 0.3$ (b) and various Péclet numbers. For the small diffusion coefficient ratio $\Delta = 3 \times 10^{-3}$, we find a gradual change in the slope of μ_{s}/μ with increasing Pe. Starting from the curve of a passive dumbbell with the dependence $\mu_{\mathrm{s}} \sim \mathrm{Wi}^{2/3}$ for $\mathrm{Wi} \gg 1$, the asymptotic dependence $\mu_{\mathrm{s}} \sim \mathrm{Wi}^{1/2}$ is assumed for $\mathrm{Pe} \to \infty$. Thereby, the asymptotic dependence $\mathrm{Wi}^{2/3}$ for $\mathrm{Wi} \to \infty$ is essentially maintained for $\mathrm{Wi} > 10^3$ and $\mathrm{Pe} < 0.1$. Note, however, that for $\mathrm{Pe} \gtrsim 1$ and $\mathrm{Wi} < \infty$, there is a large range of Weissenberg numbers, where the Lagrangian multiplier exhibits the slope $\mu_{\mathrm{s}}/\mu \approx 0.53$ before the asymptotic dependence $\sim\mathrm{Wi}^{2/3}$ is assumed.

The changes of μ_{s}/μ with increasing Péclet number are qualitatively different for $\Delta = 0.3$ compared to those for $\Delta = 3 \times 10^{-3}$. For the large Δ value, we find a gradual change from the curve of a passive dumbbell to a curve which is described by eqn (40) and is dominated by activity. For small Δ, *e.g.*, $\Delta = 3 \times 10^{-3}$, however,

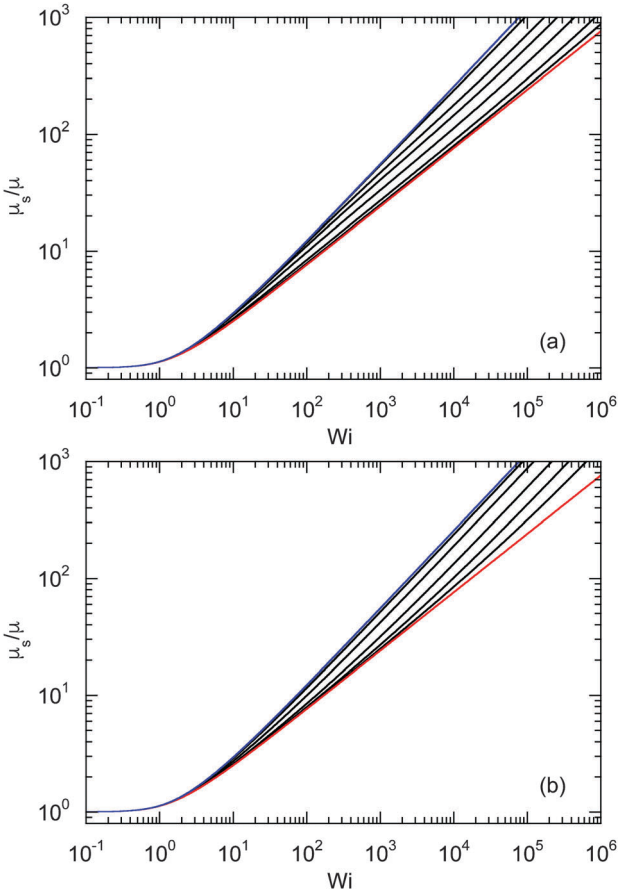

Fig. 4 Ratios of Lagrange multipliers for active dumbbells under shear flow as a function of Weissenberg number for various Péclet numbers. The ratio of the diffusion coefficients is (a) $\Delta = 3 \times 10^{-3}$ and (b) $\Delta = 3 \times 10^{-1}$. In (a), the Péclet numbers are Pe = 0 (blue), 10^{-1}, 3×10^{-1}, 5×10^{-1}, 10^0, 3×10^0, 10^1, and ∞ (red) (left to right). The Péclet numbers in (b) are Pe = 0 (blue), 1, 3, 10^1, 3×10^1, 10^2, and ∞ (red) (left to right).

we find first a gradual change of the slope to smaller values in the range $1 < \mathrm{Wi} < 10^3$ with increasing $\mathrm{Pe} < 0.1$, and then, for $\mathrm{Pe} > 0.1$, a "shift" of the whole curve to large Wi until the asymptotic behavior of eqn (40) is assumed.

4.3 Relaxation time

The nonequilibrium relaxation time τ_s follows *via* eqn (33) from the Lagrangian multiplier μ_s. Hence, it is evident that τ_s strongly depends on the Péclet number. In terms of the friction coefficient γ_R, the equation for the scaled relaxation time $\gamma_R\tau_s$ is

$$1 = 3\Delta\gamma_R\tau_s + \frac{\mathrm{Pe}^2}{2(1+\gamma_R\tau_s)}(\gamma_R\tau_s)^2 + \frac{\mathrm{Wi}^2\Delta}{2}\frac{(\gamma_R\tau_s)^3}{(\gamma_R\tau)^2} + \frac{\mathrm{Wi}^2\mathrm{Pe}^2(2+\gamma_R\tau_s)}{12(1+\gamma_R\tau_s)^2}\frac{(\gamma_R\tau_s)^4}{(\gamma_R\tau)^2} \quad (42)$$

in analogy to that of the non-sheared dumbbell in Section 3.3.

The following asymptotic dependencies are obtained:

- Pe = 0 and $\Delta < 1$

At zero Péclet number, $\mu = 1$ and $\mu_s = \mathrm{Wi}^{2/3}/\sqrt[3]{6}$. Combined with γ_R follows for $\mathrm{Pe} \ll \Delta$

$$\gamma_R\tau_s = \frac{\sqrt[3]{6}}{3\Delta\mathrm{Wi}^{2/3}}. \quad (43)$$

- $\Delta \to 0$ and $0 < \mathrm{Pe} \ll 1$

$$\gamma_R\tau_s = \frac{2\sqrt[3]{6}}{\mathrm{Pe}^2\mathrm{Wi}^{2/3}}. \quad (44)$$

- $\Delta < 1$ and $\mathrm{Pe} \ll 1$

With eqn (40)

$$\gamma_R\tau_s = \frac{2}{\mathrm{Pe}\sqrt{1+\sqrt{1+4\mathrm{Wi}^2/3}}} \xrightarrow{\mathrm{Wi}\to\infty} \frac{\sqrt[4]{12}}{\mathrm{Pe}\sqrt{\mathrm{Wi}}}. \quad (45)$$

An example of the non-equilibrium relaxation times is provided in Fig. 5 for $\Delta = 3 \times 10^{-3}$. As predicted, τ_s decreases with increasing Weissenberg number according to $\mathrm{Wi}^{-2/3}$ for $\mathrm{Pe} \lesssim 0.2$ and $\mathrm{Wi}^{-1/2}$ for $\mathrm{Pe} > 0.2$. The strong influence of activity on the relaxation time is already visible for $\mathrm{Pe} \gtrsim 0.1$ in the vicinity of $\mathrm{Wi} > 1$. Here, and even more for larger Péclet numbers, the relaxation times exhibit the dependence $\tau_s \sim \mathrm{Wi}^{-1/2}$. However, the asymptotic dependence for $\mathrm{Wi} \to \infty$ is $\gamma_R\tau_s \sim \mathrm{Wi}^{-2/3}$ as long as $\mathrm{Pe} < \infty$. In the limit $\mathrm{Pe} \to 0$, a Péclet number-independent asymptotic curve of a passive dumbbell is assumed already for $\mathrm{Pe} \lesssim 10^{-2}$. This is a consequence of the fact that Δ is finite and hence μ is equal to unity. Taking the limit $\Delta \to 0$ first yields a different behavior, where $\gamma_R\tau_s \sim \mathrm{Pe}^{-2}\mathrm{Wi}^{2/3}$ over a broad range of Péclet numbers $\mathrm{Pe} \ll 1$. Hence, the relaxation time diverges with decreasing Pe. The asymptotic dependence of eqn (40) for $\mathrm{Pe} \gg 1$ is not yet reached for Pe = 10, as reflected by the small deviation between the analytical and numerically determined curve. The plateau values for $\mathrm{Wi} \ll 1$ follow from eqn (21)

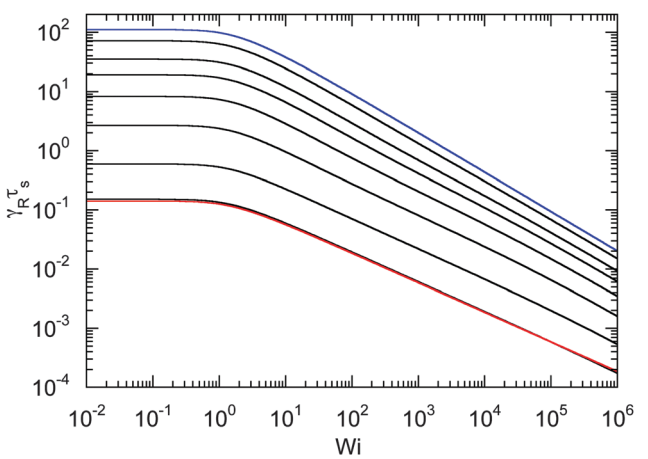

Fig. 5 Relaxation times $\gamma_R\tau_s$ as a function of Weissenberg number. The ratio of the diffusion coefficients is $\Delta = 3 \times 10^{-3}$ and the Péclet numbers are Pe = 0 (blue), 10^{-1}, 2×10^{-1}, 3×10^{-1}, 5×10^{-1}, 10^0, 3×10^0, and 10^1 (top to bottom). The curve for Pe = 0 (blue) corresponds to the solution of eqn (36) with $\mu = 1$ (see also eqn (43)). The bottom curve (red) is calculated *via* eqn (40).

4.4 Bond vector autocorrelation function

Straightforward calculations yield the bond-vector correlation functions for the Cartesian components ($t \geq 0$) (*cf.* Appendix A)

$$\langle R_y(t)R_y(0)\rangle = \left(\frac{l^2}{3\mu_s} - \frac{2v_0^2\gamma_R\tau_s^3}{3\left(1-(\gamma_R\tau_s)^2\right)}\right)e^{-t/\tau_s} + \frac{2v_0^2\tau_s^2}{3\left(1-(\gamma_R\tau_s)^2\right)}e^{-\gamma_R t}, \tag{46}$$

$$\langle R_x(t)R_x(0)\rangle = \langle R_y(t)R_y(0)\rangle + \frac{2\dot\gamma^2 v_0^2\tau_s^4}{3\left(1-(\gamma_R\tau_s)^2\right)^2}e^{-\gamma_R t} + \left[\frac{\dot\gamma^2\tau_s^2}{2}\left(\frac{l^2}{3\mu_s} - \frac{2v_0^2\gamma_R\tau_s^3}{3\left(1-(\gamma_R\tau_s)^2\right)}\right)\left(1+\frac{t}{\tau_s}\right) - \frac{2\dot\gamma^2 v_0^2\gamma_R\tau_s^5}{3\left(1-(\gamma_R\tau_s)^2\right)^2}\right]e^{-t/\tau_s}, \tag{47}$$

$$\langle R_x(t)R_y(0)\rangle = \frac{2\dot\gamma v_0^2\tau_y^3}{3(1-(\gamma_R\tau_s)^2)(1-\gamma_R\tau_s)}e^{-\gamma_R t} + \left[\frac{\dot\gamma\tau_s}{2}\left(\frac{l^2}{3\mu_s} - \frac{2v_0^2\gamma_R\tau_s^3}{3\left(1-(\gamma_R\tau_s)^2\right)}\right)\left(1+\frac{2t}{\tau_s}\right) - \frac{4\dot\gamma v_0^2\gamma_R\tau_s^4}{3\left(1-(\gamma_R\tau_s)^2\right)^2}\right]e^{-t/\tau_s}. \tag{48}$$

The bond-vector correlation function is then

$$\langle \boldsymbol{R}(t)\cdot\boldsymbol{R}(0)\rangle = \frac{2v_0^2\tau_s^2}{1-(\gamma_R\tau_s)^2}\left(1+\frac{\dot\gamma^2\tau_s^2}{3\left(1-(\gamma_R\tau_s)^2\right)}\right)e^{-\gamma_R t} + \left[l^2 + \frac{\dot\gamma^2\tau_s^2}{2}\left(\frac{l^2}{3\mu_s} - \frac{2v_0^2\gamma_R\tau_s^3}{3\left(1-(\gamma_R\tau_s)^2\right)}\right)\frac{t}{\tau_s} - \frac{2v_0^2\tau_s^2}{1-(\gamma_R\tau_s)^2}\left(1+\frac{\dot\gamma^2\tau_s^2}{3\left(1-(\gamma_R\tau_s)^2\right)}\right)\right]e^{-t/\tau_s}, \tag{49}$$

when we account for the constraint (2) and eqn (32). As for the non-sheared dumbbell, the correlation function is determined by two exponentially decaying contributions. The term including the relaxation time τ_s depends on both the Péclet number and the Weissenberg number. For $\gamma_R\tau_s \ll 1$, which follows for Pe $\gg 1$ independent of the ratio Δ, the decay of the correlation function is determined by the first term on the right-hand side of eqn (49). Here, we find $\langle \boldsymbol{R}(t)\cdot\boldsymbol{R}(0)\rangle \approx l^2 e^{-\gamma_R t}$ in the limit Wi $\gg 1$. In the opposite limit, $\gamma_R\tau_s \gg 1$, both exponential terms contribute to the relaxation for moderate shear rates.

Fig. 6 displays examples of correlation functions for various diffusion coefficient ratios, Péclet numbers, and Weissenberg numbers. For an ABDB with a very large rotational diffusion coefficient, *i.e.*, $\Delta \ll 1$ and small Pe values, both terms of eqn (49) contribute to the relaxation process. For Wi < 1, the relaxation is dominated by the second term of eqn (49) (e^{-t/τ_s}) over several orders of magnitude of the correlation function. With increasing Wi, we observe a gradual crossover to the exponential decay $l^2e^{-\gamma_R t}$ for Wi $> 10^2$. Note that even for smaller Weissenberg numbers, the long-time decay of the correlation function is given by $e^{-\gamma_R t}$. For larger Péclet numbers at the same Δ, $\gamma_R\tau_s \gg 1$ and, hence, the decay of the correlation function is dominated by the first term on the right-hand side of eqn (49). The shear-rate dependent term in the brackets dominates at large Weissenberg numbers, however, the dependence $\tau_s \sim 1/\sqrt{\text{Wi}}$ of

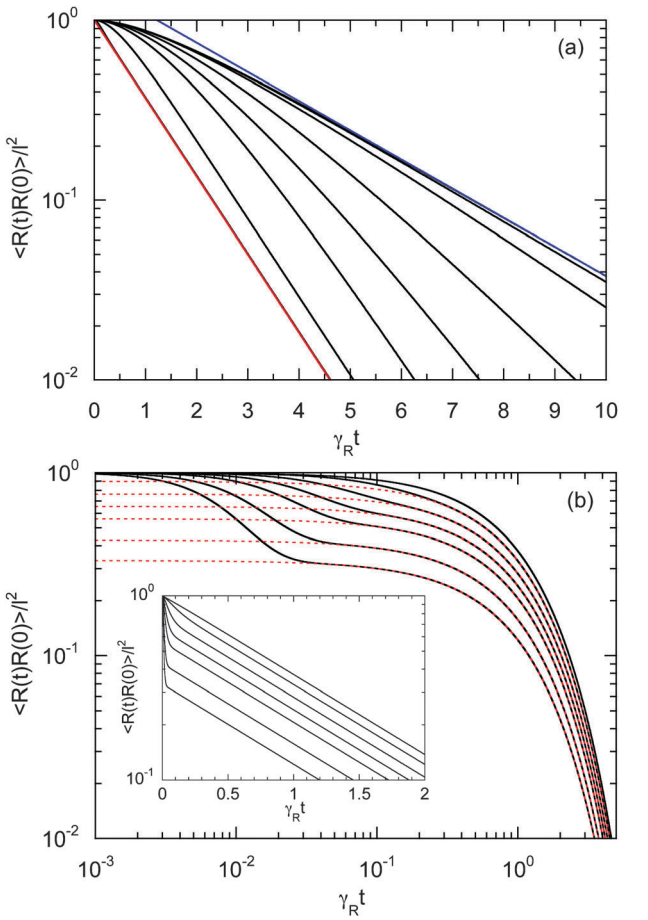

Fig. 6 Bond-vector autocorrelation functions of a dumbbell under shear flow as a function of the scaled time $\gamma_R t$ for various Weissenberg numbers. (a) Correlations are displayed for $\Delta = 3 \times 10^{-3}$, Pe = 1, and Wi = 0, 1, 2, 5, 10, 20, 100, and ∞ (red) (top to bottom). The blue line represents the exponential e^{-t/τ_s}, and the red line $e^{-\gamma_R t}$. (b) Correlations are shown for $\Delta = 3 \times 10^{-1}$, Pe = 10, and Wi = 0, 10^1, 4×10^1, 10^2, 2×10^2, 5×10^2 and 10^3 (top to bottom). The red dashed lines represent the exponential decay ($e^{-\gamma_R t}$) of the first term on the right-hand side of eqn (49). The inset shows the same curves in a semi-log representation.

the relaxation time renders the correlation function shear rate independent for these parameters.

A smaller rotational diffusion coefficient yields a clear two-state decay of the correlation function, as shown in Fig. 6(b) for $\Delta = 0.3$. In the limit $\gamma_R t \to 0$, the term with the exponential decay e^{-t/τ_s} dominates. Since $\gamma_R \tau_s < 1$, this term decays faster than the term $e^{-\gamma_R t}$. Thus, the latter term determines the long time behavior. This term is clearly shear rate dependent. Specifically for larger Weissenberg numbers, the "plateau" decreases with increasing Wi (*cf.* Fig. 6(b)). This is related to the fact that $\gamma\tau_s \sim \mathrm{Wi}^{-\kappa}$ with an exponent $\kappa > 1/2$, such that a dependence on the Weissenberg number remains, *i.e.*, $\langle \boldsymbol{R}(t)\cdot\boldsymbol{R}(0)\rangle \sim \mathrm{Wi}^{2-4\kappa}$. Note that aside from this relation, τ_s itself depends on the shear rate.

4.5 Shear-induced deformation

The correlation functions (46) and (47) yield the Cartesian components of the mean square bond vector under shear

$$\langle R_y^2\rangle = \frac{l^2}{3\mu_s} + \frac{2v_0^2\tau_s^2}{3(1+\gamma_R\tau_s)}, \tag{50}$$

$$\langle R_x^2\rangle = \langle R_y^2\rangle + \frac{l^2\dot\gamma^2\tau_s^2}{6\mu_s} + \frac{\dot\gamma^2 v_0^2\tau_s^4(2+\gamma_R\tau_s)}{3(1+\gamma_R\tau_s)^2}, \tag{51}$$

and $\langle R_z^2\rangle = \langle R_y^2\rangle$. Evidently, the gradient component $\langle R_y^2\rangle$ only depends on the shear rate *via* τ_s, whereas the flow component $\langle R_x^2\rangle$ explicitly depends on $\dot\gamma$ additionally. In terms of the Péclet number, and taking into account the constraint (2), eqn (50) and (51) become

$$\langle R_y^2\rangle = \frac{l^2}{3\mu_s} + \frac{l^2\mathrm{Pe}^2}{54\Delta^2\left(1+(3\mu_s\Delta)^{-1}\right)}\frac{1}{\mu_s^2}, \tag{52}$$

$$\langle R_x^2\rangle = l^2 - 2\langle R_y^2\rangle. \tag{53}$$

These equations depend on the Weissenberg number only implicitly *via* μ_s. Most importantly, the constraint couples the various Cartesian components of the bond vector. At zero shear, the bond orientation is isotropic, hence $\langle R_x^2\rangle = \langle R_y^2\rangle = \langle R_z^2\rangle = l^2/3$. Shear flow breaks the symmetry, and $\langle R_y^2\rangle \to 0$ for $\mathrm{Wi} \to \infty$, since $\mu_s \to \infty$ in that limit as is evident from Fig. 4. As a consequence, $\langle R_x^2\rangle \to l^2$ for $\mathrm{Wi} \to \infty$, which indicates the alignment of the dumbbell along the flow direction.

Fig. 7 provides an example of the dumbbell deformation for various Péclet numbers. For Pe = 0, eqn (50) and (51) reduce to those provided in ref. 82. Here, $\langle R_y^2\rangle$ decreases as $\mathrm{Wi}^{-2/3}$ with increasing Weissenberg number. For large Péclet numbers the second term on the right-hand side of eqn (51) dominates, and the deformation transverse to the flow direction decreases as Wi^{-1} for moderate Pe. In the asymptotic limit $\mathrm{Wi} \to \infty$, $\langle R_y^2\rangle$ decreases as $\mathrm{Wi}^{-2/3}$ with increasing Wi. As discussed in Section 4.2 in connection with the Lagrangian multiplier, a somewhat different dependence on the Weissenberg number can be observed, depending on the particular Péclet number.

The inset of Fig. 7 displays the deformation along the flow direction. Starting from the equilibrium value $l^2/3$, $\langle R_x^2\rangle$ assumes the value l^2 in the limit $\mathrm{Wi} \to \infty$, as required by the constraint (2). Thereby, the increase of $\langle R_x^2\rangle$ depends on the Péclet number, and $\langle R_x^2\rangle$ increases somewhat faster at larger Péclet numbers.

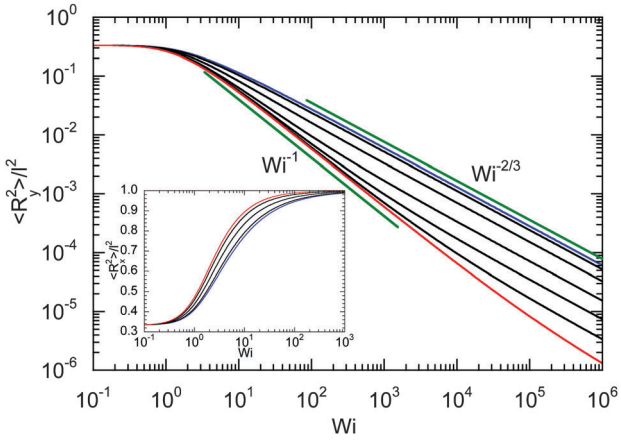

Fig. 7 Deformation transverse to the flow direction (gradient direction) of an ABDB as a function of shear rate for $\Delta = 0.3$ and the Péclet numbers Pe = 0 (blue), 1, 3, 10, 30, 100, 500, and ∞ (red) (top to bottom). The straight lines indicate the power-law decay $\mathrm{Wi}^{-2/3}$ for Pe = 0 (top) and Wi^{-1} for Pe $\to \infty$ (bottom). The inset displays the deformation along the flow direction for the Péclet numbers Pe = 0 (blue), 1, 3, 10, and ∞ (red) (right to left).

4.6 Shear-induced alignment

Shear flow implies a preferred alignment of the ABDB with respect to the flow direction, as is well known for passive polymers.[82,84,96] This alignment is characterized by the angle χ between the bond vector $\boldsymbol{R}$ and the flow direction. The angle itself is obtained from the relation

$$\tan(2\chi) = \frac{\langle R_x R_y\rangle}{\langle R_x^2\rangle - \langle R_y^2\rangle}. \tag{54}$$

Insertion of the correlations eqn (46)–(48) yields

$$\tan(2\chi) = \frac{2\mu_s}{\mathrm{Wi}\mu}, \tag{55}$$

where μ and μ_S are the solutions of eqn (19) and (34), respectively. For Pe = 0, eqn (55) reduces to the expression provided in ref. 82.

For $\mathrm{Wi} \ll 1$, $\mu_s = \mu$ and $\tan(2\chi)$ decreases as 1/Wi. The latter dependence would also apply for dumbbells/polymers with extensible bonds (Rouse/Zimm model), *i.e.*, under shear flow the polymer-contour length could increase ad infinitum. In the case of the dumbbell, this nonphysical behavior is prevented by the constraint (2). As a consequence, the alignment of finite extensible passive dumbbells is given by $\tan(2\chi) \sim \mathrm{Wi}^{-1/3}$ at large shear rates.[82,84] Activity changes the large-Weissenberg-number behavior and leads to the dependence $\tan(2\chi) \sim \mathrm{Wi}^{-1/2}$ as illustrated in Fig. 8.

Alignment is tightly linked to the rheological properties of polymers and rodlike colloids,[84,96] thus activity strongly affects the viscosity of a dilute solution of ABDBs.

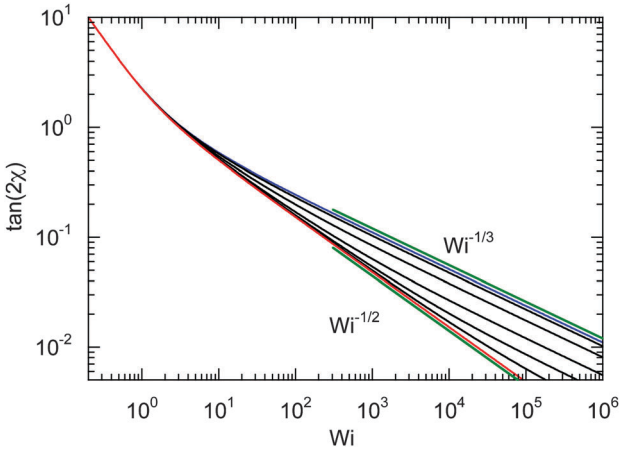

Fig. 8 Dependence of the shear-induced alignment of an ABDB [eqn (54)] on the shear rate for Δ = 0.3 and the Péclet numbers Pe = 0 (blue), 1, 3, 10, 30, 100, and ∞ (red) (top to bottom). The straight lines indicate the power-law decay $\mathrm{Wi}^{-1/3}$ for Pe = 0 (top) and $\mathrm{Wi}^{-1/2}$ for Pe $\to \infty$ (bottom).

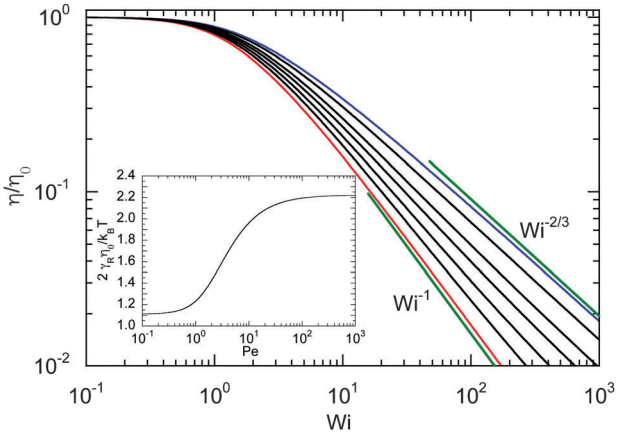

Fig. 9 Dependence of the shear viscosity of an ABDB on the shear rate for Δ = 0.3 and Pe = 0 (blue), 1, 2, 3, 5, 10, and ∞ (red) (top to bottom). The straight lines indicate the power-law decay $\mathrm{Wi}^{-2/3}$ for Pe = 0 (top) and Wi^{-1} for Pe $\to \infty$ (bottom). Inset: Zero shear viscosity (Wi = 0) as a function of Péclet number.

4.7 Shear viscosity

The shear viscosity η of a dilute solution of ABDBs follows from the relation $\eta = \sigma_{xy}/\dot{\gamma}$, where σ_{xy} is the stress tensor. The stress tensor itself is calculated from its virial representation,[58,82,83] *i.e.*,

$$\sigma_{xy} = -\frac{1}{V}\sum_{i=1}^{2}\left\langle F_{x,i}r_{y,i}\right\rangle \tag{56}$$

for a single ABDB, with the volume V of the system and the forces defined in eqn (3). The "swimm" force $\gamma_T \boldsymbol{v}_i$ does not provide a contribution to the shear stress,[58] hence, the shear stress is solely determined by the bond forces. Evaluation of the averages yields the viscosity

$$\eta = \frac{k_B T}{2V}\left(\tau_s + \frac{\gamma_T v_0^2 \tau_s^2 (2+\gamma_R\tau_s)}{3k_B T(1+\gamma_R\tau_s)^2}\right), \tag{57}$$

which explicitly and *via* τ_s depends on the propulsion velocity. The shear rate dependence enters only *via* the relaxation time. The zero-shear viscosity η_0 follows for Wi = 0, *i.e.*, τ_s has to be replaced by τ of eqn (16).

The zero-shear viscosity itself depends on the Péclet number. For Pe = 0, $\eta_0 = k_B T\tau_0/2$, or, expressed in units of γ_R,

$$\eta_0 = \frac{k_B T}{2\gamma_R}\gamma_R\tau_0 = \frac{k_B T}{6\gamma_R \Delta}. \tag{58}$$

In the asymptotic limit Pe $\to \infty$, $\gamma\tau \to \sqrt{2}/\mathrm{Pe}$, and hence, $\eta_0(\mathrm{Pe}=\infty) = 2\eta_0(\mathrm{Pe}=0)$, *i.e.*, the viscosity at large Péclet numbers is twice as large as that at zero Pe. The explicit dependence of η_0 is presented in the inset of Fig. 9. Activity evidently yields an increase of the zero shear viscosity.

The shear rate dependence of the viscosity is illustrated in Fig. 9. As expected, a dilute solution of ABDBs is shear thinning. Thereby, activity significantly affects the extent of shear thinning. For passive systems, the viscosity decreases asymptotically as $\mathrm{Wi}^{-2/3}$ at large shear rates. The slope changes gradually with increasing Péclet number, and η decreases as Wi^{-1} with increasing shear rate in the limit Pe $\to \infty$. However, already for moderate Péclet numbers on the order of $P \approx 10$, we observe a nearly linear decrease of η over a large range of shear rates.

5 Enthalpic dumbbell

As pointed out several times, the dumbbell harmonic bond (1) mimics the conformational properties of a polymer, *i.e.*, its entropic degrees of freedom, and the constraint (2) accounts for the finite polymer extensibility. In the case of an enthalpic bond, *i.e.*, a harmonic bond, where eqn (1) describes the stretching energy of the bond, no constraint exists and λ is connected to the spring constant K of the harmonic potential *via* $\lambda = K/2k_BT$. An activity and shear independent spring constant changes the conformational, dynamical, and rheological properties of the dumbbell qualitatively. Specifically, the Lagrangian multipliers obey $\lambda = \lambda_s = \lambda_0$, and thus, the relaxation times τ and τ_s are independent of activity and shear rate and are given by $\tau = \tau_s = \gamma_T/2K$. As a further consequence, $\mu = \mu_s = 1$.

For convenience, we list several of the important quantities of the enthalpic dumbbell.

(i) No shear flow

• Mean square bond vector

Without shear, eqn (15) is given by

$$\left\langle \boldsymbol{R}^2\right\rangle = \frac{3k_BT}{K}\left(1+\frac{\mathrm{Pe}^2}{6\Delta(1+\Delta Kl^2/k_BT)}\right) \tag{59}$$

in terms of the Péclet number. Evidently, the mean square bond length is affected by the activity and $\langle \boldsymbol{R}^2\rangle$ grows quadratically with Pe.

(ii) With shear flow

• Mean square bond vector transverse to the flow direction

Without constraint, the Cartesian components of any quantity are decoupled. Hence, the deformation along the gradient and vorticity directions of the mean square bond vector is

independent of the shear flow and is given by $\langle R_y^2\rangle = \langle R_z^2\rangle = \langle \boldsymbol{R}^2\rangle/3$, with $\langle \boldsymbol{R}^2\rangle$ of eqn (59).

• Mean square bond vector along the flow direction

In the direction of flow, we find

$$\langle R_x^2\rangle = \langle R_y^2\rangle + \frac{k_B T \mathrm{Wi}^2}{2K}\left[1 + \frac{\mathrm{Pe}^2}{6\Delta}\frac{1 + 2\Delta K l^2/k_B T}{(1 + \Delta K l^2/k_B T)^2}\right]. \quad (60)$$

Thus, the deformation increases quadratically with the shear rate and the bond is stretched ad infinitum with increasing Wi.

• Alignment

The bond alignment [eqn (55)] is independent of activity and decreases with increasing Weissenberg number as $\tan(2\chi) = 2/\mathrm{Wi}$.

• Viscosity

Since $\tau_s = \tau$ is independent of the shear rate, the viscosity [eqn (57)] is independent of Wi. Thus, the harmonic enthalpic dumbbell shows no shear thinning behavior. However, the viscosity depends on activity and increases quadratically with increasing Péclet number.

In summary, finite polymer extensibility leads to a drastic qualitatively different nonequilibrium behavior.

6 Summary and conclusions

We have investigated the dynamical properties of an active Brownian dumbbell, both in the absence and the presence of shear flow. The dumbbell is comprised of two active Brownian particles, which are linked by a flexible bond. The finite extensibility of the bond is captured in a mean-field manner by a prescribed mean square bond length. The latter limitation strongly couples the entropic degrees of freedom with activity and the external field. The simple model allows us to find analytical solutions for the relaxation time and the bond-vector correlation function. Both quantities strongly depend on the Péclet number. Thereby, Péclet number regimes are obtained with distinctly different dependencies on Pe for small $\Delta = D_T/l^2 D_R$, *i.e.*, large rotational diffusion coefficients.

Activity strongly affects the dynamical properties of ABDBs in shear flow. Specifically, the shear rate dependence of the relaxation time is qualitatively different from that of a passive dumbbell; it changed for $\mathrm{Wi} > 1$ from $\tau_s \sim \mathrm{Wi}^{-2/3}$ for $\mathrm{Pe} \ll 1$ to $\tau_s \sim \mathrm{Wi}^{-1/2}$ for $\mathrm{Pe} > 1$. Since the relaxation time is essentially determining the tumbling time under flow,[84] a weaker dependence of the tumbling time on the shear rate is obtained. In addition, ABDBs are better aligned with the flow, which results in a stronger shear thinning behavior and, hence, smaller viscosity at the same Weissenberg number.

In general, the obtained results highlight the effect of activity on the non-equilibrium dynamical properties of active systems with internal degrees of freedom. The dumbbell relaxation can be linked to the longest relaxation time of a polymer. Naturally, the many more internal degrees of freedom of flexible and semiflexible polymers give rise to an intricate dynamical behavior on the respective time scales, which are affected by activity. Nevertheless, we expect that the long-time behavior is captured by our dumbbell model. The dynamical aspects on shorter time scales, specifically for semiflexible polymers, remain to be elucidated. As is well known, the dynamics of long passive polymers in dilute solution is governed by hydrodynamic interactions.[79,97–99] Such interactions are absorbed in the friction coefficient for dumbbells. However, hydrodynamic interactions are expected to be important for active polymers. This is another aspect, which deserves to be considered in detail.[95]

A Bond-length constraint and bond vector correlation functions

A.1 Bond length constraint

In the stationary state, the bond-length constraint (15) is given by

$$\langle \boldsymbol{R}^2\rangle = \int_{-\infty}^{t}\int_{-\infty}^{t} \mathrm{e}^{-2t/\tau}\mathrm{e}^{(t'+t'')/\tau} \times \langle[\Delta\boldsymbol{v}(t') + \Delta\boldsymbol{\Gamma}(t')]\cdot[\Delta\boldsymbol{v}(t'') + \Delta\boldsymbol{\Gamma}(t'')]\rangle \mathrm{d}t'\mathrm{d}t'' \quad (61)$$

in terms of the solution (12) of the equation of motion (11). The correlation functions of the random variables $\Delta\boldsymbol{v}$ and $\Delta\boldsymbol{\Gamma}$ follow as

$$\langle \Delta\boldsymbol{\Gamma}(t)\cdot\Delta\boldsymbol{\Gamma}(t')\rangle = 12\gamma_T k_B T\delta(t - t'), \quad (62)$$

$$\langle \Delta\boldsymbol{\nu}(t)\cdot\Delta\boldsymbol{\nu}(t')\rangle = 2v_0^2\mathrm{e}^{-\gamma_R|t - t'|}. \quad (63)$$

Insertion of these correlation functions leads to

$$\langle \boldsymbol{R}^2\rangle = \int_{-\infty}^{t}\int_{-\infty}^{t} \mathrm{e}^{-2t/\tau}\mathrm{e}^{(t'+t'')/\tau} \times \left[2v_0^2\mathrm{e}^{-\gamma_T|t'-t''|} + \frac{12k_B T}{\gamma}\delta(t' - t'')\right]\mathrm{d}t'\mathrm{d}t''. \quad (64)$$

Evaluation of the integrals yields eqn (15).

A.2 Bond vector correlation function: no shear

The bond vector correlation function (23) is obtained in a similar fashion. In terms of the solution (12) of the equations of motion, the correlation function reads

$$\langle \boldsymbol{R}(t)\cdot\boldsymbol{R}(0)\rangle = \int_{-\infty}^{t}\int_{-\infty}^{0} \mathrm{e}^{-t/\tau}\mathrm{e}^{(t'+t'')/\tau} \times \langle[\Delta\boldsymbol{v}(t') + \Delta\boldsymbol{\Gamma}(t')]\cdot[\Delta\boldsymbol{v}(t'') + \Delta\boldsymbol{\Gamma}(t'')]\rangle \mathrm{d}t'\mathrm{d}t''. \quad (65)$$

The calculation of the correlation functions of the random forces leads to

$$\langle \boldsymbol{R}(t)\cdot\boldsymbol{R}(0)\rangle = \int_{-\infty}^{t}\int_{-\infty}^{0} \mathrm{e}^{-t/\tau}\mathrm{e}^{(t'+t'')/\tau} \times \left[2v_0^2\mathrm{e}^{-\gamma_T|t'-t''|} + \frac{12k_B T}{\gamma}\delta(t' - t'')\right]\mathrm{d}t'\mathrm{d}t''. \quad (66)$$

Evaluation of the integrals and insertion of eqn (2) yield eqn (23) and (24).

A.3 Bond vector correlation function: shear

Under shear, the bond vector correlation function along the shear direction is

$$\langle R_x(t)R_x(0)\rangle = \int_{-\infty}^{t}\int_{-\infty}^{0} \mathrm{e}^{-t/\tau}\mathrm{e}^{(t'+t'')/\tau}\big\langle\left[\Delta v_x(t') + \Delta\Gamma_x(t') + \dot\gamma R_y(t')\right] \times \left[\Delta v_x(t'') + \Delta\Gamma_x(t'') + \dot\gamma R_y(t'')\right]\big\rangle \mathrm{d}t'\mathrm{d}t''.$$

Inserting the correlation functions of the random variables, the correlation function becomes

$$\langle R_x(t)R_x(0)\rangle = \int_{-\infty}^{t}\int_{-\infty}^{0} \mathrm{e}^{-t/\tau}\mathrm{e}^{(t'+t'')/\tau}\left[\frac{2}{3}v_0{}^2\mathrm{e}^{-\gamma_\mathrm{T}|t'-t''|} + \frac{4k_\mathrm{B}T}{\gamma}\delta(t'-t'') + \dot\gamma^2\big\langle R_y(t')R_y(t'')\big\rangle\right]\mathrm{d}t'\mathrm{d}t''. \quad (67)$$

Since the correlation functions along the gradient and vorticity directions are unaffected by shear flow, they are given by the respective Cartesian components of eqn (66), hence

$$\langle R_x(t)R_x(0)\rangle = \frac{1}{3}\langle \boldsymbol{R}(t)\cdot\boldsymbol{R}(0)\rangle + \frac{\dot\gamma^2}{3}\int_{-\infty}^{t}\int_{-\infty}^{0}\mathrm{e}^{-t/\tau}\mathrm{e}^{(t'+t'')/\tau}\langle \boldsymbol{R}(t')\cdot\boldsymbol{R}(t'')\rangle\mathrm{d}t'\mathrm{d}t''. \quad (68)$$

The correlation function $\langle \boldsymbol{R}(t')\cdot\boldsymbol{R}(t'')\rangle$ follows from eqn (23) with the argument $|t'-t''|$, *i.e.*, t is replaced by $|t'-t''|$. Finally, eqn (46)–(48) follow by integration.

Acknowledgements

Helpful discussions with Thomas Eisenstecken and the financial support of the project by the DFG within the priority program SPP 1726 "Microswimmers" are gratefully acknowledged.

References

1 J. Elgeti, R. G. Winkler and G. Gompper, *Rep. Prog. Phys.*, 2015, **78**, 056601.
2 M. F. Copeland and D. B. Weibel, *Soft Matter*, 2009, **5**, 1174.
3 N. C. Darnton, L. Turner, S. Rojevsky and H. C. Berg, *Biophys. J.*, 2010, **98**, 2082.
4 D. B. Kearns, *Nat. Rev. Microbiol.*, 2010, **8**, 634–644.
5 K. Drescher, J. Dunkel, L. H. Cisneros, S. Ganguly and R. E. Goldstein, *Proc. Natl. Acad. Sci. U. S. A.*, 2011, **10940**, 108.
6 J. D. Partridge and R. M. Harshey, *J. Bacteriol.*, 2013, **195**, 909.
7 J. Bialké, T. Speck and H. Löwen, *Phys. Rev. Lett.*, 2012, **108**, 168301.
8 I. Buttinoni, J. Bialké, F. Kümmel, H. Löwen, C. Bechinger and T. Speck, *Phys. Rev. Lett.*, 2013, **110**, 238301.
9 B. M. Mognetti, A. Šarić, S. Angioletti-Uberti, A. Cacciuto, C. Valeriani and D. Frenkel, *Phys. Rev. Lett.*, 2013, **111**, 245702.
10 I. Theurkauff, C. Cottin-Bizonne, J. Palacci, C. Ybert and L. Bocquet, *Phys. Rev. Lett.*, 2012, **108**, 268303.
11 Y. Fily, S. Henkes and M. C. Marchetti, *Soft Matter*, 2014, **10**, 2132.
12 X. Yang, M. L. Manning and M. C. Marchetti, *Soft Matter*, 2014, **10**, 6477.
13 J. Stenhammar, D. Marenduzzo, R. J. Allen and M. E. Cates, *Soft Matter*, 2014, **10**, 1489.
14 Y. Fily, A. Baskaran and M. F. Hagan, *Soft Matter*, 2014, **10**, 5609.
15 G. S. Redner, M. F. Hagan and A. Baskaran, *Phys. Rev. Lett.*, 2013, **110**, 055701.
16 Y. Fily and M. C. Marchetti, *Phys. Rev. Lett.*, 2012, **108**, 235702.
17 R. Großmann, L. Schimansky-Geier and P. Romanczuk, *New J. Phys.*, 2012, **14**, 073033.
18 V. Lobaskin and M. Romenskyy, *Phys. Rev. E: Stat., Nonlinear, Soft Matter Phys.*, 2013, **87**, 052135.
19 A. Zöttl and H. Stark, *Phys. Rev. Lett.*, 2014, **112**, 118101.
20 A. Wysocki, R. G. Winkler and G. Gompper, *EPL*, 2014, **105**, 48004.
21 H. C. Berg, *E. Coli in Motion*, Springer, 2004.
22 S. Ramaswamy, *Annu. Rev. Condens. Matter Phys.*, 2010, **1**, 323.
23 F. J. Nédélec, T. Surrey, A. C. Maggs and S. Leibler, *Nature*, 1997, **389**, 305.
24 J. Howard, *Mechanics of motor proteins and the cytoskeleton*, Sinauer Associates Sunderland, MA, 2001.
25 K. Kruse, J. F. Joanny, F. Jülicher, J. Prost and K. Sekimoto, *Phys. Rev. Lett.*, 2004, **92**, 078101.
26 A. R. Bausch and K. Kroy, *Nat. Phys.*, 2006, **2**, 231.
27 F. Jülicher, K. Kruse, J. Prost and J.-F. Joanny, *Phys. Rep.*, 2007, **449**, 3.
28 Y. Harada, A. Noguchi, A. Kishino and T. Yanagida, *Nature*, 1987, **326**, 805.
29 V. Schaller, C. Weber, C. Semmrich, E. Frey and A. R. Bausch, *Nature*, 2010, **467**, 73.
30 M. C. Marchetti, J. F. Joanny, S. Ramaswamy, T. B. Liverpool, J. Prost, M. Rao and R. A. Simha, *Rev. Mod. Phys.*, 2013, **85**, 1143.
31 J. Prost, F. Jülicher and J.-F. Joanny, *Nat. Phys.*, 2015, **11**, 111.
32 T. Vicsek and A. Zafeiris, *Phys. Rep.*, 2012, **517**, 71.
33 J. R. Howse, R. A. L. Jones, A. J. Ryan, T. Gough, R. Vafabakhsh and R. Golestanian, *Phys. Rev. Lett.*, 2007, **99**, 048102.
34 G. Volpe, I. Buttinoni, D. Vogt, H. J. Kümmerer and C. Bechinger, *Soft Matter*, 2011, **7**, 8810.
35 Y. Mei, A. A. Solovev, S. Sanchez and O. G. Schmidt, *Chem. Soc. Rev.*, 2011, **40**, 2109.
36 B. ten Hagen, F. Kümmel, R. Wittkowski, D. Takagi, H. Löwen and C. Bechinger, *Nat. Commun.*, 2014, **5**, 4829.
37 B. Scharf, *J. Bacteriol.*, 2002, **184**, 5979.
38 A. Cordoba, J. D. Schieber and T. Indei, *RSC Adv.*, 2014, **4**, 17935.
39 Y. Sumino, K. H. Nagai, Y. Shitaka, D. Tanaka, K. Yoshikawa, H. Chate and K. Oiwa, *Nature*, 2012, **483**, 448.
40 S. Kim and S. J. Karrila, *Microhydrodynamics: principles and selected applications*, Butterworth-Heinemann, Boston, 1991.
41 E. Lauga and T. R. Powers, *Rep. Prog. Phys.*, 2009, **72**, 096601.

42 K. Drescher, R. E. Goldstein, N. Michel, M. Polin and I. Tuval, *Phys. Rev. Lett.*, 2010, **105**, 168101.
43 J. S. Guasto, K. A. Johnson and J. P. Gollub, *Phys. Rev. Lett.*, 2010, **105**, 168102.
44 N. Watari and R. G. Larson, *Biophys. J.*, 2010, **98**, 12.
45 J. Hu, M. Yang, G. Gompper and R. G. Winkler, *Soft Matter*, 2015, **11**, 7843.
46 S. Ghose and R. Adhikari, *Phys. Rev. Lett.*, 2014, **112**, 118102.
47 G. S. Klindt and B. M. Friedrich, *Phys. Rev. E: Stat., Nonlinear, Soft Matter Phys.*, 2015, **92**, 063019.
48 F. Peruani, L. Schimansky-Geier and M. Bär, *Eur. Phys. J.: Spec. Top.*, 2010, **191**, 173.
49 P. Romanczuk, M. Bär, W. Ebeling, B. Lindner and L. Schimansky-Geier, *Eur. Phys. J.: Spec. Top.*, 2012, **202**, 1.
50 M. Yang and M. Ripoll, *Soft Matter*, 2014, **10**, 1006.
51 A. P. Solon, J. Stenhammar, R. Wittkowski, M. Kardar, Y. Kafri, M. E. Cates and J. Tailleur, *Phys. Rev. Lett.*, 2015, **114**, 198301.
52 A. P. Solon, Y. Fily, A. Baskaran, M. E. Cates, Y. Kafri, M. Kardar and J. Tailleur, *Nat. Phys.*, 2015, **11**, 673.
53 S. C. Takatori, W. Yan and J. F. Brady, *Phys. Rev. Lett.*, 2014, **113**, 028103.
54 C. Maggi, U. M. B. Marconi, N. Gnan and R. Di Leonardo, *Sci. Rep.*, 2015, **5**, 10742.
55 F. Ginot, I. Theurkauff, D. Levis, C. Ybert, L. Bocquet, L. Berthier and C. Cottin-Bizonne, *Phys. Rev. X*, 2015, **5**, 011004.
56 E. Bertin, *Physics*, 2015, **8**, 44.
57 T. Speck, A. M. Menzel, J. Bialké and H. Löwen, *J. Chem. Phys.*, 2015, **142**, 224109.
58 R. G. Winkler, A. Wysocki and G. Gompper, *Soft Matter*, 2015, **11**, 6680.
59 T. Vicsek, A. Czirók, E. Ben-Jacob, I. Cohen and O. Shochet, *Phys. Rev. Lett.*, 1995, **75**, 1226.
60 H. H. Wensink and H. Löwen, *Phys. Rev. E: Stat., Nonlinear, Soft Matter Phys.*, 2008, **78**, 031409.
61 Y. Yang, V. Marceau and G. Gompper, *Phys. Rev. E: Stat., Nonlinear, Soft Matter Phys.*, 2010, **82**, 031904.
62 M. Abkenar, K. Marx, T. Auth and G. Gompper, *Phys. Rev. E: Stat., Nonlinear, Soft Matter Phys.*, 2013, **88**, 062314.
63 D. Loi, S. Mossa and L. F. Cugliandolo, *Soft Matter*, 2011, **7**, 10193.
64 A. Ghosh and N. S. Gov, *Biophys. J.*, 2014, **107**, 1065.
65 R. E. Isele-Holder, J. Elgeti and G. Gompper, *Soft Matter*, 2015, **11**, 7181.
66 T. B. Liverpool, A. C. Maggs and A. Ajdari, *Phys. Rev. Lett.*, 2001, **86**, 4171.
67 D. Sarkar, S. Thakur, Y.-G. Tao and R. Kapral, *Soft Matter*, 2014, **10**, 9577.
68 R. Chelakkot, A. Gopinath, L. Mahadevan and M. F. Hagan, *J. R. Soc., Interface*, 2013, **11**, 20130884.
69 G. Jayaraman, S. Ramachandran, S. Ghose, A. Laskar, M. S. Bhamla, P. B. S. Kumar and R. Adhikari, *Phys. Rev. Lett.*, 2012, **109**, 158302.
70 A. Laskar, R. Singh, S. Ghose, G. Jayaraman, P. B. S. Kumar and R. Adhikari, *Sci. Rep.*, 2013, **3**, 1964.
71 H. Jiang and Z. Hou, *Soft Matter*, 2014, **10**, 1012.
72 J. P. Hernandez-Ortiz, C. G. Stoltz and M. D. Graham, *Phys. Rev. Lett.*, 2005, **95**, 204501.
73 V. B. Putz, J. Dunkel and J. M. Yeomans, *Chem. Phys.*, 2010, **375**, 557.
74 A. Furukawa, D. Marenduzzo and M. E. Cates, *Phys. Rev. E: Stat., Nonlinear, Soft Matter Phys.*, 2014, **90**, 022303.
75 C. Valeriani, M. Li, J. Novosel, J. Arlt and D. Marenduzzo, *Soft Matter*, 2011, **7**, 5228.
76 A. Suma, G. Gonnella, D. Marenduzzo and E. Orlandini, *EPL*, 2014, **108**, 56004.
77 L. F. Cugliandolo, G. Gonnella and A. Suma, *Phys. Rev. E: Stat., Nonlinear, Soft Matter Phys.*, 2015, **91**, 062124.
78 A. Suma, G. Gonnella, G. Laghezza, A. Lamura, A. Mossa and L. F. Cugliandolo, *Phys. Rev. E: Stat., Nonlinear, Soft Matter Phys.*, 2014, **90**, 052130.
79 R. B. Bird, C. F. Curtiss, R. C. Armstrong and O. Hassager, *Dynamics of Polymer Liquids*, John Wiley & Sons, New York, 1987, vol. 2.
80 A. Puliafito and K. Turitsyn, *Phys. D*, 2005, **211**, 9.
81 Y.-G. Tao, I. O. Götze and G. Gompper, *J. Chem. Phys.*, 2008, **128**, 144902.
82 B. Kowalik and R. G. Winkler, *J. Chem. Phys.*, 2013, **138**, 104903.
83 R. G. Winkler and P. Reineker, *Macromolecules*, 1992, **25**, 6891.
84 R. G. Winkler, *Soft Matter*, 2010, **6**, 6183.
85 R. G. Winkler, *J. Chem. Phys.*, 2010, **133**, 164905.
86 M. G. Bawendi and K. F. Freed, *J. Chem. Phys.*, 1985, **83**, 2491.
87 R. A. Harris and J. E. Hearst, *J. Chem. Phys.*, 1966, **44**, 2595.
88 W. Carl, *Macromol. Theory Simul.*, 1996, **5**, 1.
89 F. Ganazzoli, G. Allegra, E. Colombo and M. D. Vitis, *Macromolecules*, 1995, **28**, 1076.
90 M. Dolgushev, T. Guérin, A. Blumen, O. Bénichou and R. Voituriez, *J. Chem. Phys.*, 2014, **141**, 014901.
91 J. Saragosti, P. Silberzan and A. Buguin, *PLoS One*, 2012, **7**, e35412.
92 S. Tavaddod, M. A. Charsooghi, F. Abdi, H. R. Khalesifard and R. Golestanian, *Eur. Phys. J. E: Soft Matter Biol. Phys.*, 2011, **34**, 1.
93 H. Risken, *The Fokker-Planck Equation*, Springer, Berlin, 1989.
94 P. Hänggi and P. Jung, *Adv. Chem. Phys.*, 1995, **89**, 239.
95 A. Kaiser, S. Babel, B. ten Hagen, C. von Ferber and H. Löwen, *J. Chem. Phys.*, 2015, **142**, 124905.
96 C.-C. Huang, R. G. Winkler, G. Sutmann and G. Gompper, *Macromolecules*, 2010, **43**, 10107.
97 M. Doi and S. F. Edwards, *The Theory of Polymer Dynamics*, Clarendon Press, Oxford, 1986.
98 L. Harnau, R. G. Winkler and P. Reineker, *J. Chem. Phys.*, 1996, **104**, 6355.
99 E. P. Petrov, T. Ohrt, R. G. Winkler and P. Schwille, *Phys. Rev. Lett.*, 2006, **97**, 258101.